# Low-loss fiber-to-chip couplers with ultrawide optical bandwidth  (EP)

H. Gehring, M. Blaicher, W. Hartmann, P. Varytis, K. Busch, M. Wegener, and W. H. P. Pernice

## COLLECTIONS

(EP)  This paper was selected as an Editor's Pick

View Online    Export Citation    CrossMark

## ARTICLES YOU MAY BE INTERESTED IN

Realizing $Q > 300\,000$ in diamond microdisks for optomechanics via etch optimization
APL Photonics **4**, 016101 (2019); https://doi.org/10.1063/1.5053122

Why I am optimistic about the silicon-photonic route to quantum computing
APL Photonics **2**, 030901 (2017); https://doi.org/10.1063/1.4976737

Enhanced magneto-optical effects in hybrid Ni-Si metasurfaces
APL Photonics **4**, 016102 (2019); https://doi.org/10.1063/1.5066307

# Low-loss fiber-to-chip couplers with ultrawide optical bandwidth (EP)

View Online    Export Citation    CrossMark

H. Gehring,[1,a)] M. Blaicher,[2,a),b)] W. Hartmann,[1] P. Varytis,[3] K. Busch,[3,4] M. Wegener,[5,6] and W. H. P. Pernice[1,c)]

### AFFILIATIONS

[1] Institute of Physics, University of Münster, Wilhelm-Klemm-Str. 10, 48149 Münster, Germany
[2] Institute of Microstructure Technology (IMT), Karlsruhe Institute of Technology (KIT), Hermann-von-Helmholtz-Platz 1, 76344 Eggenstein-Leopoldshafen, Germany
[3] Humboldt-Universität zu Berlin, Institut für Physik, AG Theoretische Optik & Photonik, Newtonstr. 15, 12489 Berlin, Germany
[4] Max-Born-Institut, Max-Born-Str. 2A, 12489 Berlin, Germany
[5] Institute of Nanotechnology, Karlsruhe Institute of Technology (KIT), 76021 Karlsruhe, Germany
[6] Institute of Applied Physics, Karlsruhe Institute of Technology (KIT), 76128 Karlsruhe, Germany

[a)] H. Gehring and M. Blaicher contributed equally to this work.
[b)] **Now at:** Nanoscribe GmbH, Hermann-von-Helmholtz-Platz 1, 76344 Eggenstein-Leopoldshafen, Germany.
[c)] **Author to whom correspondence should be addressed:** wolfram.pernice@uni-muenster.de

### ABSTRACT

Providing efficient access from optical fibers to on-chip photonic systems is a key challenge for integrated optics. In general, current solutions allow either narrowband out-of-plane-coupling to a large number of devices or broadband edge-coupling to a limited number of devices. Here we present a hybrid approach using 3D direct laser writing, merging the advantages of both concepts and enabling broadband and low-loss coupling to waveguide devices from the top. In the telecom wavelength regime, we demonstrate a coupling loss of less than –1.8 dB between 1480 nm and 1620 nm. In the wavelength range between 730 nm and 1700 nm, we achieve coupling efficiency well above –8 dB which is sufficient for a range of broadband applications spanning more than an octave. The 3D couplers allow relaxed mechanical alignment with respect to optical fibers, with –1 dB alignment tolerance of about 5 $\mu$m in x- and y-directions and –1 dB alignment tolerance in the z-direction of 34 $\mu$m. Using automatized alignment, many such couplers can be connected to integrated photonic circuits for rapid prototyping and hybrid integration.

Integrated photonic circuits provide significant advantages in terms of functionality, component cost, and scalability which are particularly attractive for miniaturizing complex optical systems. In the field of optical data communication, such devices have enabled a continuous increase in data rates,[1] and integrated optical circuits have been used extensively for biosensing[2] and lab-on-a-chip systems.[3] They have also found profound interest in the field of integrated quantum optics.[4,5] In such circuits, numerous optical components are joined into complete systems using waveguides which act as the optical analog to electrical wires in integrated electrical circuits. Besides light routing across the chip surface, waveguides further enable near-field coupling to nanoscale components and thus provide an optical interface to nanosystems. Based on this approach, high-efficiency single-photon detectors have been developed[6,7] as well as integrated single-photon sources[8] where waveguide access holds promise for scalable fabrication.

For all of these applications, high-efficiency coupling to optical fibers is desirable and necessary to achieve compatibility with the existing telecommunication infrastructure, which plays a major role especially in integrated data communication. Fiber access enables joining individual circuit systems into distributed networks and allows for testing and convenient device readout. Besides providing access to photonic

chips from a macroscopic world and providing multi-terminal access to multiple waveguides, a wide optical bandwidth is essential for multiplexed data communication. Similarly, in optical quantum technologies and integrated quantum optical circuits, optically pumping single-photon sources and collecting the generated photons equally requires a wide bandwidth. In addition, in such experiments achieving high coupling efficiencies is essential, for performing experiments where photon loss is detrimental. For multi-photon experiments in integrated quantum optics, low coupling loss is crucial, as the event detection count rate scales with the product of all coupling efficiencies. Low coupling loss is equally essential in all classical photonic applications and thus a key metric for fiber-to-chip coupling structures. Therefore, a significant effort has been devoted for developing efficient coupling architectures which bridge the gap from a rather macroscopic optical fiber to a nanoscale waveguide.

In a broad sense, coupling to integrated waveguides is performed by direct coupling either from the chip facet if high efficiencies or a wide optical bandwidth is the most important parameter or from the top if addressing many devices or a less time-consuming fabrication is desired. In both approaches, matching the size of the device mode to the size of the fiber-mode is essential for achieving high coupling efficiencies. The mode-size conversion can be performed either on the chip using tapering structures[9–15] or off-chip using lensed fibers,[16] tapered fibers,[17–21] or a lens between the chip and the fiber.[22] High coupling efficiencies have been shown using direct coupling from the chip facet.[23] Recently, printing of microlenses by direct laser writing (DLW)[24] onto the facets of the chip has been introduced, allowing to efficiently couple standard single mode fibers to on-chip waveguides and thus relaxing the alignment procedure.[25] Alternatively, tapered waveguides, which connect to a fiber attached to the chip, have been used,[26] thus enabling computer-aided alignment of the structures. Likewise, freestanding waveguides fabricated by DLW have further been used for interconnecting InP-lasers with silicon waveguide circuits.[27]

Nevertheless, edge-coupling limits the number of addressable devices on a chip as the photonic components either need to be placed near the chip edges or have to be routed to the edges using bus waveguides in a non-intersecting fashion. Furthermore, spot size converters which allow for mode matching between a bus waveguide and a fiber are rather large. Therefore, for addressing many devices, e.g., for parameter-scans during development and for rapid prototyping, out-of-plane coupling from the top of the chip is preferred. This approach requires changing the direction in which light is propagating. Most planar approaches employ periodic structures, e.g., grating couplers, which reflect the light upwards.[28,29] Since this coupling scheme depends on the periodicity of the grating, it is typically optimized for a certain polarization and wavelength and thus broadband coupling is challenging.[30,31] Because grating devices can be fabricated during waveguide realization, grating couplers are very suitable for scalable chip access and for addressing many photonic

elements. Using inverse design, the efficiency of grating couplers has been predicted to approach near-unity[32] and also could enable vertical emission. For wide optical bandwidth, however, relying on interference effects in grating structures is not ideal and thus adiabatic solutions are preferred. In the telecom region, this has been shown in Ref. 33 using a low-refractive index oil/cladding material with silicon photonic waveguides. However, for very broadband applications covering both visible and near-infrared wavelength regimes, waveguide solutions with higher optical bandwidth are required.

Here we present a hybrid approach for coupling from the top by using near-adiabatic-mode-converters which are laid out in three dimensions without the need for a cladding material. We employ 3D direct laser writing (DLW) for fabricating polymer waveguide-to-fiber couplers which are free from planar design restrictions. Using DLW, continuous bending of the polymer waveguide is possible and thus removes the need for periodic structures. Furthermore, DLW also allows for the free design of the waveguide and thus enables free variation of its shape and size as well as beam shaping elements like lenses at the end of the waveguide. Using automatized alignment with respect to planar integrated photonic circuits, we demonstrate a low coupling loss of –1.8 dB in the telecommunication band and ultrawide bandwidth from visible wavelengths to the near infrared. Our approach allows for connecting many waveguide devices to optical fibers with micrometer scale alignment tolerances inherent to the mode field size of a single mode fiber. These structures hold promise for rapid prototyping in photonics and for compact out-of-plane coupling to broadband filter architectures and optical sources.

An overview of the proposed coupling device is shown schematically in Fig. 1(a). Here the 3D polymer coupler (blue) is used to rotate the direction of the incoming light into the planar direction and to convert the mode field diameter of an optical fiber to the size of a nanophotonic waveguide (orange). For mechanical support, the coupling architecture is equipped with two support tethers [left in Fig. 1(a)] which do not significantly disturb optical propagation through the polymer. The coupling device is connected to planar waveguides which also provide wide optical bandwidth at visible and infrared wavelengths. We use silicon nitride waveguides with a nominal thickness of 340 nm and a width of 1.3 $\mu$m to support only a single transverse electric (TE)-mode at telecommunication wavelengths.

The polymer coupler [see blue structure in Fig. 1(a)] starts on a chip with an adiabatic transition from a single mode silicon nitride waveguide to the polymer waveguide over a length of 20 $\mu$m.[34] In order to expand the optical mode, the width of the silicon nitride waveguide is decreased linearly from 1.3 $\mu$m to 0.02 $\mu$m in the tapering region, while simultaneously the height of the surrounding polymer waveguide covering the taper is increased from zero to 2 $\mu$m, keeping the width constant at 2 $\mu$m, in order to allow an adiabatic transition
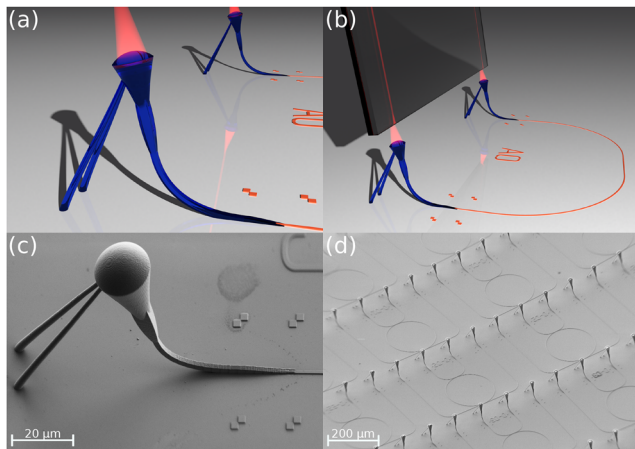
**FIG. 1**. (a) Rendering of a polymer coupler (blue) attached to a silicon nitride waveguide (orange). The double-square-markers used for alignment are also shown. (b) Rendering of the hybrid photonic circuit for carrying out transmission tests. A fiber array with a pitch of 250 $\mu$m is placed over the couplers. Both couplers are connected by a silicon nitride single mode waveguide. (c) SEM-micrograph of a fabricated coupler realized by DLW. (d) SEM-micrograph of a photonic chip with several devices illustrating scalable fabrication of hybrid 3D-planar photonic circuits.

between the fundamental TE-modes of the two waveguides. At telecommunication wavelengths, the polymer waveguide only supports the fundamental TE- and TM (transverse magnetic)-mode as long as the waveguide is still residing on the silicon oxide. In this work, we attach these coupling structures to silicon nitride nanophotonic circuits. Because of the design approach, however, there should not be fundamental limits for attaching the couplers to other photonic platforms such as silicon-on-insulator,[35] diamond-on-insulator, or aluminum nitride-on-insulator although the taper dimensions should be adjusted for each specific material.

Following the tapering region, the waveguide is lifted from the chip using an out-of-plane bend. The bending continues until the polymer waveguide has reached an angle of 12° with respect to the vertical direction. This angle corresponds to the free-space diffraction direction of an 8°-polished-fiber-array which we employ for determining the insertion loss [see Fig. 1(b)]. The angle-polished fiber-array allows for addressing multiple grating couplers on a chip arranged in a row. To avoid the excitation of higher modes, the curvature is continuously changed allowing a smooth transition. The couplers can easily be adapted for other fiber angles by changing the bend structure. The fibers used for the measurements are standard telecom fibers (Corning SMF28) with a mode field diameter of 10.4 $\mu$m at a wavelength of 1550 nm and a cutoff wavelength of higher fiber modes at 1260 nm.

After the bending region, a transition from the rectangular shape to a round shape is incorporated to match the coupler to the rotational symmetry of the fiber. The shape is initially described by a 2 $\mu$m square and finally by a circle with a diameter of 21 $\mu$m. Over a length of 50 $\mu$m, the shape

is continuously altered. After this transition region, a spherical lens with a curvature of 12 $\mu$m is added to the front of the polymer waveguide to focus the outgoing beam. To compensate for the mechanical torque which this structure would have with respect to the lifting point on the chip surface, two supporting tethers were added at the front of the structure [see Fig. 1(c)]. We find experimentally that these support structures lead only to minimal scattering loss and do not affect the coupling efficiency significantly. Through numerical simulations, the initial coupler structure is optimized for emitting a beam whose beam waist matches the mode-field-diameter of the used single mode fiber of 10.4 $\mu$m at a wavelength of 1550 nm [see Fig. 3(d)]. This device geometry is then experimentally optimized using multiple fabricated structures as outlined in the following.

To experimentally assess the optical performance of the polymer couplers, we realize hybrid planar-3D photonic structures using a combination of planar lithography and DLW. Planar lithography is used for fabricating on-chip waveguides and photonic circuits, while DLW is subsequently used to attach 3D couplers to the waveguide devices. For measuring the transmission spectrum of these couplers, a fiber-array and two-terminal devices, as shown in Fig. 1(b), are used. In this design, light is coupled into on-chip waveguides with the first coupler, propagates through the photonic circuit, and is coupled out again with a second 3D coupler. Since the silicon-nitride waveguides show a low propagation loss of 0.2 dB/cm at telecommunication wavelengths as determined by us previously,[36] this calibration circuit allows for characterizing the transmission spectrum of the 3D couplers. The first fabrication step consists of fabricating the planar waveguides and alignment structures. Starting with a silicon nitride [340 nm thick, commercially grown by low pressure chemical vapor deposition (LPCVD)] thin film on a silicon dioxide (3.3 $\mu$m thick) layer on silicon, a negative-tone resist (ma-N 2403) is spin coated and exposed using electron-beam-lithography (Raith EBPG5150). Afterwards, the resist is developed in MF-319 (Microposit) and subsequent dry etching in fluorine chemistry using a mixture of $CHF_3$ and $O_2$ is performed. Finally, the resist is removed using oxygen plasma cleaning. The fabrication process is explained in more detail in our previous work.[36]

In a second step, the here presented couplers are written by using dip-in DLW (Nanoscribe Professional GT, 63× objective) onto the existing planar structures using IP-Dip (Nanoscribe) as a resist.[37] The IP-Dip resist provides a refractive index of 1.52 at a wavelength of 780 nm according to the manufacturer (Nanoscribe) and thus moderate refractive index contrast against the silicon dioxide substrate. For precise alignment, double-square-markers which are realized in parallel with the photonic waveguides [see Fig. 1(c)] are used. The positions of these markers are determined automatically using pattern recognition from a camera image of the chip. From the positions of the markers, the precise location of the polymer taper within the 3D structure is calculated. After aligning the model of the coupler to match the corresponding waveguide taper, the structures are written

slice-by-slice in the z-direction with slices of 100 nm and a hatching distance (distance between the written lines in lateral dimension) of 100 nm as well. The slicing distance leads to the residual scale-like structures visible in Fig. 1. However, as both chosen values are well below the writing resolution of the Nanoscribe DLW system, these distances lead to a low surface roughness after development. By decreasing these distances, the surface roughness could be improved further. Because the wavelength of the light at telecommunication wavelengths is well above the chosen distances, the improvement of the insertion loss is expected to be insignificantly low. Using the described resolution, each coupler needs about 8 min of writing time and the couplers are fabricated in a fully automated way [see many successively automatically fabricated couplers in Fig. 1(d)]. Finally, the structures are developed in propylene glycol monomethyl ether acetate (PGMEA) for 5 min, removing the unexposed resist, rinsed with isopropanol, and blown dry with a nitrogen-gun. The mechanical support structures of the couplers give the design sufficient mechanical stability that during wet processing, the couplers do not collapse and do not require critical point drying. With this fabrication method described above, we realize many different coupling structures on a chip in order to scan the design parameters described above.

Due to the adiabatic design, the 3D couplers possess broad coupling bandwidth, covering both visible wavelengths and the near-infrared wavelength regime. To characterize the transmission performance of the coupling device, we perform two different measurements. First, to determine the transmission properties in the telecom wavelength range, the fiber array is connected to a polarized tunable laser source [Santec TSL-710 (blue)/TSL-510 (orange)], a polarization controller and a power-meter (Newport 2011-FC). Second, in order to carry out broadband transmission spectrum measurement, the fiber array is connected to a supercontinuum white-light-source (Leukos SM-30-450) and an optical spectrum analyzer (Ando AQ6317b).

The results of the measurements are depicted in Fig. 2 for an optimized coupling geometry with best performance. The measurements are taken for a pair of 3D couplers attached to a single waveguide, as shown in the schematic rendering of Fig. 1(b). Assuming reciprocity of the photonic circuit, from the total transmission, we extract the spectral properties of a single coupler by taking the square root of the measured spectrum in a linear scale. First, using the two tunable laser sources with the complementary wavelength range, the transmission through the entire circuit was measured after optimizing the polarization of the laser to maximize the transmission as the
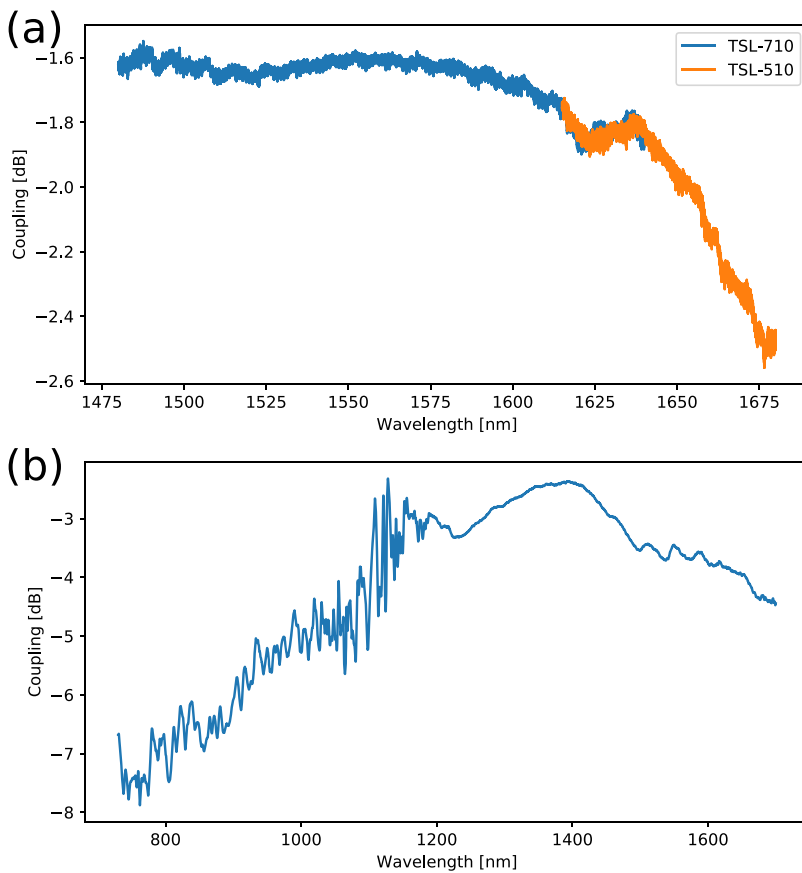


FIG. 2. Transmission spectra of a coupler. (a) Transmission measured using two tunable laser sources. The range from 1480 nm to 1640 nm is measured using a Santec TSL-710 tunable laser source, and the range from 1610 nm to 1680 nm is measured using a Santec TSL-510 tunable laser source. For both ranges, a Newport Model 2011 detector is used. (b) Transmission measured using a circular polarized white-light-source (Leukos SM-30-450) and an optical spectrum analyzer (Ando AQ6317b).

planar silicon nitride waveguide supports only the fundamental TE-mode in this region. The coupler shows broadband transmission in the telecom wavelength regime where the additional insertion loss with respect to the minimal value remains below −1 dB over range of more than 200 nm [see Fig. 2(a)]. The couplers do not show optical degradation when illuminated with conventional telecommunication lasers combined with power amplification up to 100 mW and retain their performance over periods of several months without change.

In addition, using the supercontinuum source, the optical transmission in the range from 730 nm to 1700 nm was measured. As shown in Fig. 2(b), each coupler has an insertion loss of less than −8 dB over the entire measured wavelength range which exceeds one octave (i.e., a factor of two in wavelength). Because the white-light source is unpolarized, a part of the light in the telecom region is lost as the waveguide is designed to be single mode in this region. Hence, only the TE-portion of the light from the white light source is coupled into the on-chip devices, while the TM-part is rejected by the waveguide. Therefore, this measurement shows lower transmission in comparison with the tunable laser source by roughly 1.5 dB in the telecommunication range. For lower wavelengths (~1300 nm), the silicon nitride waveguide also supports the TM-mode, resulting in a higher transmission. For wavelengths below 1260 nm, the fiber supports multiple modes, leading to a less flat spectrum and more insertion loss. In order to determine the reproducibility of the coupling efficiency of the presented scheme, we fabricated 19 devices with an identical design, consisting of a pair of couplers connected via an on-chip waveguide. These structures showed an average coupling efficiency of −2.07 dB with a standard deviation of 0.35 dB at a wavelength of 1550 nm.

To determine the additional insertion loss due to misalignment of the 3D couplers with respect to the fiber array, high precision linear stages (PI Q545) are used for exact positioning in the x-, y-, and z-directions. We map out the coupling loss into the waveguides by moving the couplers relative to the fiber array in two orthogonal area scans. As shown in the 2D-profiles in Fig. 3 measured at a wavelength of 1550 nm, the couplers offer relaxed alignment tolerances. In the x-/y-direction, the −1 dB range amounts to about 5 $\mu$m, which fits to the predictions made by the overlap integral between two shifted Gaussian modes with a mode field diameter of 10.4 $\mu$m (Corning SMF-28).

In the z-direction, a displacement of 34 $\mu$m leads to an additional insertion loss of −1 dB which is a result of the beam focus provided by the polymer lens terminating the 3D coupler. This property is also confirmed by finite-difference time-domain (FDTD) simulations, as shown in Fig. 3(d), for which an extrapolation of the dispersion relation of IP-Dip[38] is used (~1.53 at a wavelength of ~1550 nm). The scan along the x-axis shown in Fig. 3(c) shows the Gaussian profile of the emitted beam. The shape of the measured curve fits well to the Gaussian given by the overlap integral over two modes with a mode field diameter of 10.4 $\mu$m which equals the mode field diameter of the used SMF-28 fiber. Because of the relaxed alignment tolerances, the optical noise performance of the devices is comparable with standard grating coupling structures.
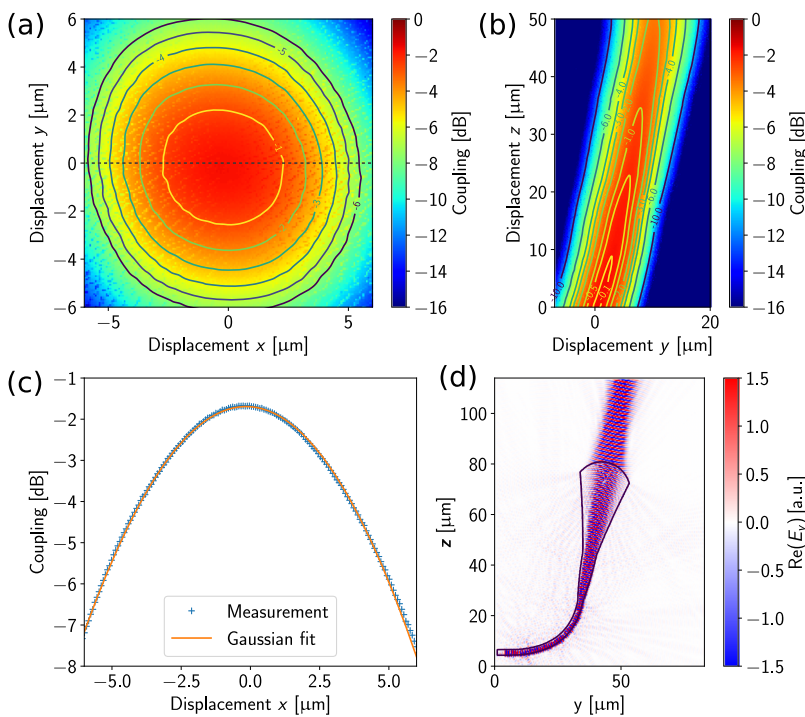


FIG. 3. (a) Dependence of the coupler transmission on the alignment in the x- and y-directions. (b) Alignment tolerance measured in the y- and z-directions, showing focused emission from the coupler. (c) Cross-sectional alignment tolerance in the x-direction, taken along the line indicated in (a). A Gaussian is fitted to the profile. (d) FDTD simulation of the 3D couplers at a wavelength of 1550 nm using MEEP.
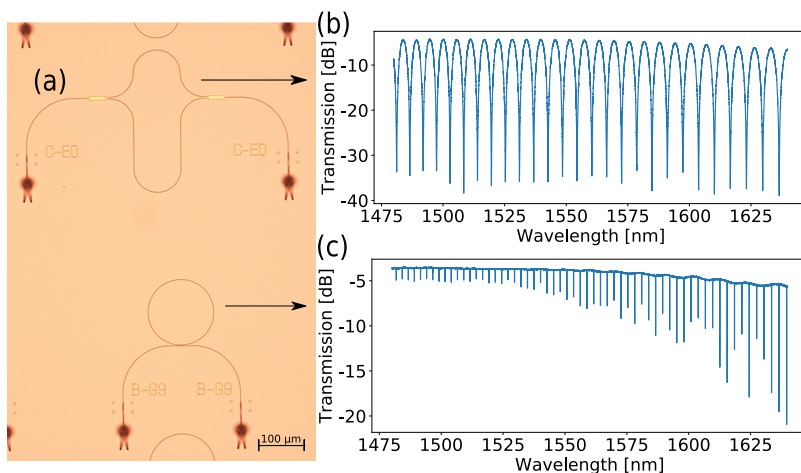
**FIG. 4**. (a) Optical micrograph of 3D couplers attached to two different PICs. (b) Transmission spectrum of a PIC consisting of two 3D couplers and a Mach Zehnder interferometer (MZI). (c) Transmission spectrum of a PIC consisting of two 3D couplers and a ring resonator.

Besides offering wide optical bandwidth and good alignment tolerances, the 3D couplers can be attached to multi-terminal devices using automatized marker search and alignment. This way photonic circuits with multiple elements can be conveniently read out with out-of-plane optical access. In Fig. 4, we show exemplary measurements with different photonic integrated circuits (PICs), namely, circuits containing a ring-resonator and a Mach-Zehnder interferometer. Both photonic components show a broad optical response over many free spectral ranges and thus benefit from the broadband coupling bandwidth of the 3D couplers. As expected, one can observe in Fig. 4(b) the typical Mach-Zehnder interference fringes over a broad wavelength range. In Fig. 4(c), the typical dips of the ring resonator over the whole range are clearly visible, separated by the free-spectral range of the resonator. Furthermore, as the transmission spectrum of the couplers is fairly flat in the telecommunication band, the spectrum is hardly superimposed by residual effects, as for example Fabry-Pérot interferences which would arise due to back reflections from the couplers, which is often a problem with conventional grating couplers.

In conclusion, we have presented an approach for contact-free optical coupling from standard single-mode fibers from the top of the chip to planar photonic circuitry using 3D devices realized by state-of-the-art direct laser writing. The couplers offer a flat transmission spectrum over a broad wavelength range and do not depend on periodic structures by exploiting near-adiabatic tapering. Besides the high coupling bandwidth, the design also offers a low insertion loss. By adjusting the final radius of the waveguide and the curvature of the lens, the couplers can be further optimized for other wavelength regions, e.g., to match to single mode fibers in the visible wavelength range.

Because our coupling concept combines high efficiency, a wide optical bandwidth, and good alignment tolerances, it facilitates rapid prototyping for broadband photonic applications, e.g., spectrometers and nonlinear optical devices such as frequency-combs or second-harmonic generation sources.

The coupling concept can also be readily adapted for on-chip quantum-optical experiments, allowing in-coupling of the pump light and out-coupling of the generated single photons through the same coupler. Furthermore, our concept is applicable for packaging purposes, where multiple fibers, e.g., in a fiber array, have to be permanently attached to a nanophotonic chip.

## REFERENCES

[1] J. Pfeifle, V. Brasch, M. Lauermann, Y. Yu, D. Wegner, T. Herr, K. Hartinger, P. Schindler, J. Li, D. Hillerkuss, R. Schmogrow, C. Weimann, R. Holzwarth, W. Freude, J. Leuthold, T. J. Kippenberg, and C. Koos, Nat. Photonics **8**, 375 (2014).

[2] C. A. Barrios, M. J. Bañuls, V. González-Pedro, K. B. Gylfason, B. Sánchez, A. Griol, A. Maquieira, H. Sohlström, M. Holgado, and R. Casquel, Opt. Lett. **33**, 708 (2008).

[3] M. C. Estevez, M. Alvarez, and L. M. Lechuga, Laser Photonics Rev. **6**, 463 (2012).

[4] X. Qiang, X. Zhou, J. Wang, C. M. Wilkes, T. Loke, S. O'Gara, L. Kling, G. D. Marshall, R. Santagati, T. C. Ralph, J. B. Wang, J. L. O'Brien, M. G. Thompson, and J. C. F. Matthews, Photon. **12**, 534 (2017).

[5] J. Wang, S. Paesani, Y. Ding, R. Santagati, P. Skrzypczyk, A. Salavrakos, J. Tura, R. Augusiak, L. Mančinska, D. Bacco, D. Bonneau, J. W. Silverstone, Q. Gong, A. Acín, K. Rottwitt, L. K. Oxenløwe, J. L. O'Brien, A. Laing, and M. G. Thompson, Science **360**, 285 (2018).

[6] O. Kahl, S. Ferrari, V. Kovalyuk, G. N. Goltsman, A. Korneev, and W. H. P. Pernice, Sci. Rep. **5**, 10941 (2015).

[7] C. Schuck, W. H. P. Pernice, and H. X. Tang, Appl. Phys. Lett. **102**, 051101 (2013).

[8] P. Schnauber, J. Schall, S. Bounouar, T. Höhne, S. I. Park, G. H. Ryu, T. Heindel, S. Burger, J. D. Song, S. Rodt, and S. Reitzenstein, Nano Lett. **18**, 2336 (2018).

[9] V. R. Almeida, R. R. Panepucci, and M. Lipson, Opt. Lett. **28**, 1302 (2003).

[10] R. M. Reano and P. Sun, Proc. SPIE **7606**, 76060J (2010).

[11] K. Shiraishi, H. Yoda, and C. S. Tsai, Opt. Express **20**, 024370 (2012).

[12] A. Khilo, M. A. Popović, M. Araghchini, and F. X. Kärtner, Opt. Express **18**, 015790 (2010).

[13] H. Park, S. Kim, J. Park, J. Joo, and G. Kim, Opt. Express **21**, 029313 (2013).

[14] K.-N. Ku and M.-C. M. Lee, in Optical Fiber Communication Conference/National Fiber Optic Engineers Conference 2013 (OSA, 2013), Vol. 1, p. OTu2C.3.

[15] R. H. Khandokar, M. Bakaul, M. Asaduzzaman, A. Nirmalathas, and S. Skafidas, IEEE J. Quantum Electron. **52**(9), 8400106 (2016).

[16] G. Ren, S. Chen, Y. Cheng, and Y. Zhai, Opt. Commun. **284**, 4782 (2011).

[17] C. P. Michael, M. Borselli, T. J. Johnson, C. Chrystal, and O. Painter, Opt. Express **15**, 4745 (2007).

[18] S. Gröblacher, J. T. Hill, A. H. Safavi-Naeini, J. Chan, and O. Painter, Appl. Phys. Lett. **103**, 181104 (2013).

[19] T. G. Tiecke, K. P. Nayak, J. D. Thompson, T. Peyronel, N. P. de Leon, V. Vuletić, and M. D. Lukin, Optica **2**, 70 (2014).

[20] R. S. Daveau, K. C. Balram, T. Pregnolato, J. Liu, E. H. Lee, J. D. Song, V. Verma, R. Mirin, S. W. Nam, L. Midolo, S. Stobbe, K. Srinivasan, and P. Lodahl, Optica **4**, 178 (2016).

[21] M. J. Burek, C. Meuwly, R. E. Evans, M. K. Bhaskar, A. Sipahigil, S. Meesala, B. MacHielse, D. D. Sukachev, C. T. Nguyen, J. L. Pacheco, E. Bielejec, M. D. Lukin, and M. Lončar, Phys. Rev. Appl. **8**, 024026 (2017).

[22] L. Chang, M. Dijkstra, N. Ismail, M. Pollnau, R. M. de Ridder, K. Wörhoff, V. Subramaniam, and J. S. Kanger, Opt. Express **23**, 022414 (2015).

[23] M. Pu, L. Liu, H. Ou, K. Yvind, and J. M. Hvam, Opt. Commun. **283**, 3678 (2010).

[24] J. Fischer and M. Wegener, Laser Photonics Rev. 7, 22 (2013).

[25] P. Dietrich, M. Blaicher, I. Reuter, M. R. Billah, T. Hoose, A. Hofmann, C. Caer, R. Dangel, B. Offrein, U. Troppenz, M. Moehrle, W. Freude, and C. Koos, Nat. Photonics **12**, 241 (2018).

[26] N. Lindenmann, S. Dottermusch, M. L. Goedecke, T. Hoose, M. R. Billah, T. P. Onanuga, A. Hofmann, W. Freude, and C. Koos, J. Lightwave Technol. **33**, 755 (2015).

[27] M. R. Billah, M. Blaicher, T. Hoose, P.-I. Dietrich, P. Marin-Palomo, N. Lindenmann, A. Nesic, A. Hofmann, U. Troppenz, M. Moehrle, S. Randel, W. Freude, and C. Koos, Optica **5**, 876 (2018).

[28] M. L. Dakss, L. Kuhn, P. F. Heidrich, and B. A. Scott, Appl. Phys. Lett. **16**, 523 (1970).

[29] G. Roelkens, D. Van Thourhout, and R. Baets, Opt. Lett. **32**, 1495 (2007).

[30] Z. Xiao, T.-Y. Liow, J. Zhang, P. Shum, and F. Luan, Opt. Express **21**, 5688 (2013).

[31] Q. Zhong, V. Veerasubramanian, Y. Wang, W. Shi, D. Patel, S. Ghosh, A. Samani, L. Chrostowski, R. Bojko, and D. V. Plant, Opt. Express **22**, 018224 (2014).

[32] A. Michaels and E. Yablonovitch, Opt. Express **26**, 4766 (2018).

[33] M. Blaicher, M. R. Billah, T. Hoose, P.-I. Dietrich, A. Hofmann, S. Randel, W. Freude, and C. Koos, in Conference on Lasers and Electro-Optics, 2018, STh1A.1.

[34] M. Schumann, T. Bückmann, N. Gruhler, M. Wegener, and W. Pernice, Light: Sci. Appl. **3**, e175 (2014).

[35] N. Lindenmann, G. Balthasar, D. Hillerkuss, R. Schmogrow, M. Jordan, J. Leuthold, W. Freude, and C. Koos, Opt. Express **20**, 017667 (2012).

[36] N. Gruhler, C. Benz, H. Jang, J.-H. Ahn, R. Danneau, and W. H. P. Pernice, Opt. Express **21**, 031678 (2013).

[37] T. Bückmann, N. Stenger, M. Kadic, J. Kaschke, A. Frölich, T. Kennerknecht, C. Eberl, M. Thiel, and M. Wegener, Adv. Mater. **24**, 2710 (2012).

[38] T. Gissibl, S. Wagner, J. Sykora, M. Schmid, and H. Giessen, Opt. Mater. Express **7**, 2293 (2017).